

Division of chemically active droplet as protocell paradigm is modeled by the diffusion equation with a negative coefficient

Mohammad Abu Hamed^{1,2}

¹*Department of Mathematics, Technion - Israel Institute of Technology, Haifa 32000, Israel*

²*Department of Mathematics, The College of Sakhnin - Academic College for Teacher Education, Sakhnin 30810, Israel*

It has been suggested recently that growth and division of a protocell could be modeled by a chemical active droplet with simple chemical reactions driven by an external fuel supply, thus proposing a key for understanding the early steps of life origin, this model is called the continuum model. Indeed it's numerical simulation manifests a shape instability which results in droplet division into two smaller droplets of equal size resembling cell division [1]. In this paper, we investigate the linear version of the continuum model, which is called the effective model. This model is formulated in the plain and studied both in the linear and nonlinear regime. First, we perform a linear stability analysis for the flat interface, and then we develop a nonlinear theory following Sivashinsky method [2] in the limit of the small supersaturation number. We find that the interface at the leading order is governed by the diffusion equation with a negative coefficient, and an exact solution is obtained when a Gaussian initial condition is considered, thus shedding light on the nature of the division phenomena of an active droplet both in time and space. The formulation and solution of the corresponding three dimensional problem are straightforward.

I. INTRODUCTION

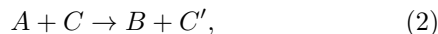
How did the first cell emerge from primitive precursors i.e., "Protocell"? and what is a protocell made of? These are central questions about the origin of life. In 1924, Oparin suggested that a protocell could be a liquid droplet without membrane; its interface segregates two coexisting phases and many substances could diffuse across the interface [3], therefore, the droplet's volume could produce some chemical reactions. However, the questions about how droplets replicate, grow, and divide remain unexplained.

Recently, the work of [1] suggests an answer, where they introduce a simple model that includes a phase separation of a droplet material B surrounded by a dilute material A . These materials undergo chemical reactions driven by an external fuel supply that keeps the system away from thermodynamic equilibrium. Such a droplet is called a chemical active droplet.

We explain the kinetics of such a simple chemical reaction cycle as follow: the chemical potential $\mu(B)$ of the droplet molecules is higher than $\mu(A)$ of the dilute molecules, therefore inside the droplet, we have the spontaneous chemical reaction



Molecules A are soluble, hence they leave the droplet and move to the dilute phase. For the backward direction, we have the reaction,



where the new material C , the fuel and C' the product preserves the constant chemical potential difference $\Delta\mu(C) = \mu(C) - \mu(C') > 0$ in order to maintain the system out of thermal equilibrium. Finally, material B diffuses inside the droplet thus completing the reaction cycle, see Fig 3.

The combination of the chemical reactions (1) and (2), the phase separation by a sharp interface, and the fuel supply to maintain nonequilibrium, are described by the continuum model. This model was solved numerically in Ref. [1], and indeed it exhibits a shape instability of the spherical active droplet which results in the elongation of the interface to form a dumbbell shape until it splits into two smaller daughter droplets of equal size resembling cell division. Note that this is an unusual behavior since the surface tension which often opposes any deviation from spherical shape is suppressed.

It is worth to compare this model with other less simple models for spontaneous droplet division, such as the one in Ref. [4] for investigating the mechanics of nematic active droplet; in Ref. [5], by considering the negative surface tension; in Ref. [6] where they consider the PH changes and the electrostatic contribution to the interface free energy; and in Ref. [7] by considering the elastic property of the two sided membrane interface.

When investigating the stability of the spherical active droplet in Ref. [1], they consider the linearized version of the continuum model which is called the effective model. Depending on the droplet's radius and the supersaturation parameter $N^+ > 0$, see (11), that represent the excess concentration of the droplet material far from the droplet, they observe three different scenarios that an active droplet may undergo, (i) the droplet shrink until it disappears, this is called size instability (unstable state), (ii) the droplet grows toward stationary radius where the influx is balanced by the efflux across the interface, and therefore it coexists with the surrounding (stable state), (iii) the droplet may undergo shape instability where any small shape deformation triggers the elongation along one axis until droplet division (unstable state).

All of the previous models for droplet spontaneous division where investigated and solved numerically in the post linear (nonlinear) regime. As far as we know, there are no analytical results in the framework of the nonlinear

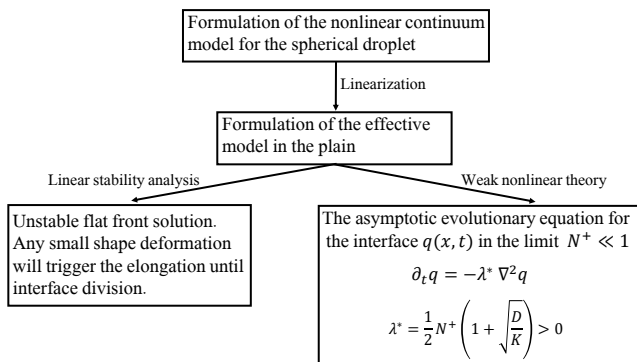


FIG. 1. A flowchart that describes the main structure and results of the paper.

theory for the dynamics of active droplet, therefore the main goal of this paper is to introduce the first analytical result in the nonlinear regime, where we derive an asymptotic evolutionary equation that governs only the droplet interface dynamics in the limit of the small supersaturation number $N^+ \ll 1$, by following Sivashinsky method [2] which is considered one of the basic achievements of the nonlinear theory of the morphological instability. A flow chart is introduced for describing the paper's main structure and results, see Fig. 1.

The paper is organized as follows. In Sec. II, we formulate both the continuum and effective model in the space, and we formulate the effective model in the plain. In Sec. III, we analyze the linear stability for the one dimensional flat interface. In Sec. IV, an asymptotic close evolutionary equation for the interface dynamics is derived in the limit of long waves, and a Gaussian initial condition is considered. In Sec. V, we revisit the generalization of the previous sections to the two dimensional interface considering only the end results.

II. FORMULATION OF THE PROBLEM

In the next two subsections, we will introduce the continuum and effective models that were developed in the supplementary information (SI) of Ref. [1].

A. Description of the continuum model

Consider an incompressible fluid that includes a droplet phase material B with concentration $u(\vec{r}, t)$ in the ocean of a dilute phase material A , where its concentration is determined from the incompressibility condition [8]. The two phases are strongly segregated by a sharp interface, therefore following ideas from Ref. [9] we consider the double well free energy density function

$$f(u) = \frac{b}{2(\Delta u)^2} (u - u_-^{(0)})^2 (u - u_+^{(0)})^2$$

which describes the two coexisting liquid phases, where $u_-^{(0)}$ and $u_+^{(0)}$ are the equilibrium concentrations of material B in the droplet and dilute phases respectively, separated by a flat interface. The positive parameter b characterizes the molecular interactions and entropic contributions, and $\Delta u = |u_-^{(0)} - u_+^{(0)}|$.

The state of the system is described by the free energy functional

$$F[u] = \int_V \left(f(u) + \frac{\kappa}{2} |\nabla u|^2 \right) dv,$$

where V is the volume of the system, dv is a volume element, and κ is a coefficient concerning the surface tension and the interface width [9]. Consequently, the chemical potential is given by the variational derivative,

$$\mu = \frac{\delta F}{\delta u} = \frac{b}{|\Delta u|^2} (u - u_-^{(0)}) (u - u_+^{(0)}) (2u - u_-^{(0)} - u_+^{(0)}) - \kappa \nabla^2 u.$$

Hence, the material concentration field dynamics is governed by the reaction diffusion equation,

$$u_t = m \nabla^2 \mu + s(u), \quad (3)$$

where m is a mobility coefficient of the droplet material B , and the reaction function $s(u)$ is designed to be linear in the phases outside and inside the droplet, and smoothly interpolated by a cubic polynomial $p_3(u)$ in some interval $u_c^- < u < u_c^+$, where u_c^\pm are some characteristic concentration, see Fig. (2),

$$s(u) = \begin{cases} \nu^+ + k^+(u_+^{(0)} - u), & u \leq u_c^+, \\ p_3(u), & u_c^- \leq u \leq u_c^+, \\ -\nu^- + k^-(u_-^{(0)} - u), & u_c^- \leq u, \end{cases} \quad (4)$$

here k^\pm are the reaction rate outside and inside the droplet respectively, and similarly ν^\pm are the reaction fluxes at equilibrium concentration, notice that the polynomial $p_3(u)$ is uniquely determined.

Considering the sharp interface limit between phases, equation (3) is appended with two boundary conditions at the interface. The first is the continuity of the chemical potential across the interface,

$$\mu(u^-) = \mu(u^+), \quad (5)$$

and the second is the Laplace pressure jump discontinuity across the interface,

$$(u^- - u^+) \mu(u^-) + f(u^+) - f(u^-) = 2\gamma H, \quad (6)$$

where γ is the surface tension or the free energy per unit of area of the interface, and H is the local mean curvature of the interface. Equations (5) and (6) are the coexistence conditions of the inside and outside phases that are separated by the droplet interface [10], [8]. Notice that u^- and u^+ in equations (5) and (6) are the concentration evaluated at the interface inside and outside the droplet, respectively.

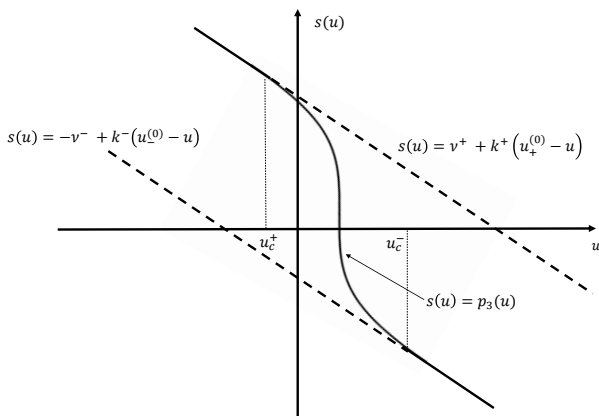


FIG. 2. Description of the source function $s(u)$ in (4) that behaves as cubic when $u_c^- < u < u_c^+$ and linear otherwise.

B. The effective model as a linear approximation of the continuum model

In order to perform a linear stability analysis to our system, we need to formulate a linear version of the continuum model of the previous section. Therefore, the source function (4) is approximated to linear order by,

$$s^L(u) = \begin{cases} \nu^+ + k^+(u_+^{(0)} - u), & \text{outside the droplet,} \\ -\nu^- + k^-(u_-^{(0)} - u), & \text{inside the droplet,} \end{cases} \quad (7)$$

notice that for the concentration $u = -\nu^-/k^- + u_-^{(0)}$, the reaction flux inside the droplet vanishes, and for the concentration $u = \nu^+/k^+ + u_+^{(0)}$, the reaction flux outside the droplet vanishes. Next, we will refer the signs (+) and (-) for the value outside and inside the droplet, respectively.

Linearizing the concentration u in equation (3) at the values $u_-^{(0)}$ and $u_+^{(0)}$ inside and outside the droplet respectively yields the linear equations,

$$\partial_t u^\pm = D^\pm \nabla^2 u^\pm - m^\pm \kappa \nabla^4 u^\pm + s^L(u), \quad (8)$$

where u^+ and u^- are the concentration of the droplet material B outside and inside the droplet respectively, and D^\pm are the corresponding diffusion coefficients.

We remind that the bi-harmonic terms $m^\pm \kappa \nabla^4 u^\pm$ in equations (8) were omitted in the formulation of the effective model in Ref. [1] since the characteristic interface width is small compared to the spherical droplet radius, and the concentration variations are typically small away from the interface where the "reaction diffusion" equations (8) hold. In this paper, we investigate equations (8) in close proximity to the interface while assuming that the interface width $6\gamma\beta/\Delta u$ is small enough in comparison to the diffusion length $L^+ = \sqrt{D^+/k^+}$ (SI [1]) i.e.,

$$\frac{6\gamma\beta}{\Delta u} \ll \sqrt{\frac{D^+}{k^+}}, \quad (9)$$

therefore we adopt the same approximation also here and the bi-harmonic terms will be neglected next.

Also, recall that the diffusion coefficient is related to the mobility coefficient by the relation $D = mb$, but the diffusion coefficient D^\pm in equations (8) for the effective model is different in the two phases, while the mobility coefficient m in equation (3) for the continuum model is uniformly constant in both phases. This could be explained as follows, usually, the mobility coefficient depends on the local environment, i.e., $m = m(u)$, thus leading to a concentration dependent diffusivity which can be approximated as constant in each phase D^\pm [8]. Now the assumption that m is uniformly constant in the continuum model is rather technical in order to reduce the number of parameters, thus simplifying the numerical simulations (SI [1]).

In the small surface tension limit, $\gamma \ll \Delta u/(H\beta)$, where $\beta = 2/(b\Delta u)$ is the coefficient that describes the Laplace pressure effect on the interface's concentration, the equilibrium conditions (5) and (6) are approximated as follows,

$$\begin{aligned} u^- &\sim u_-^{(0)} + \beta\gamma H, \\ u^+ &\sim u_+^{(0)} + \beta\gamma H. \end{aligned}$$

The interface dynamics are governed by

$$v_n = \hat{\mathbf{n}} \cdot \frac{\mathbf{j}^- - \mathbf{j}^+}{u^- - u^+}, \quad (10)$$

where v_n is the normal velocity of the interface, $\hat{\mathbf{n}}$ is unit vector normal to the interface, and $\mathbf{j}^\pm = -D^\pm \nabla u^\pm$ are the diffusion fluxes outside and inside the droplet, respectively. Recall again that u^\pm in (10) are the concentrations evaluated outside and inside the droplet interface, respectively.

C. Formulation of the nondimensional problem in the plain

Both the continuum and the effective models of the previous sections were studied in the framework of a spherical droplet in a spherical coordinate system centered at the droplet center (SI [1]). In this paper, we consider a cross section of a spherical droplet, and then we concentrate (zoom in) on the region where the division occurs, see Fig. (3). In that region, we may formulate the effective model in the infinite plain with cartesian coordinate (x, y) , consequently, the whole spherical droplet dynamics are reduced to the dynamics of a one dimensional interface that could be described by the function $y = q(x, t)$, Fig. (3). The goal of the next sections is to understand the dynamics of such interface using only analytical tools both in the linear and post linear regime in comparison with [1] where they perform only numerical simulations in the nonlinear regime.

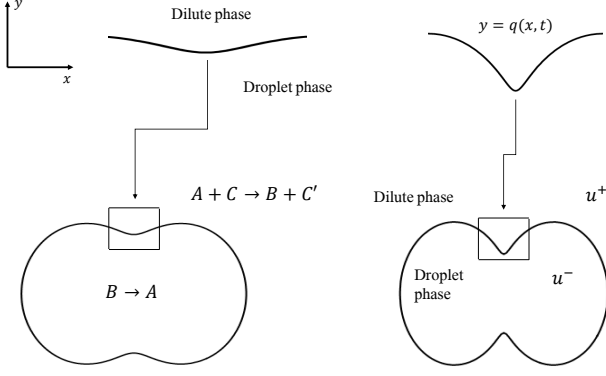


FIG. 3. A schematic description of the droplet division dynamics while concentrating (zooming in) on the region where the division occurs. In addition, we add a description of the chemical reaction cycle where inside, the droplet material B is spontaneously transformed into soluble dilute material A that leaves the droplet. Then outside, the droplet material A is transformed into material B coupled with chemical fuel C and product C' . Lastly material B diffuses inside the droplet, thus completing the reaction cycle.

We begin with the formulation of the plain effective model in a nondimensional form. Consider the concentration, length, and time scale respectively,

$$\Delta u = u_-^{(0)} - u_+^{(0)}, \quad L^+ = \sqrt{\frac{D^+}{k^+}}, \quad T^+ = \frac{1}{k^+},$$

then we define the scaled variables and fields,

$$\begin{aligned} (x, y) &= L^+(x^*, y^*), \quad t = T^+ t^*, \\ u(x, y, t) &= (\Delta u) u^{**}(L^+ x^*, L^+ y^*, T^+ t^*) = \\ &= (\Delta u) u^*(x^*, y^*, t^*), \\ q(x, t) &= L^+ q^{**}(L^+ x^*, T^+ t^*) = L^+ q^*(x^*, t^*), \\ H(x, t) &= (L^+)^{-1} H^{**}(L^+ x^*, T^+ t^*) = (L^+)^{-1} H^*(x^*, t^*). \end{aligned}$$

As a result, we obtain seven nondimensional parameters of the system,

$$\begin{aligned} N^\pm &= \frac{\nu^\pm}{k^+ \Delta u}, \quad U^- = \frac{u_-^{(0)}}{\Delta u}, \quad B^\pm = \frac{\beta^\pm \gamma}{L^+ \Delta u}, \\ D &= \frac{D^-}{D^+}, \quad K = \frac{k^-}{k^+}. \end{aligned} \quad (11)$$

Denote $U^+ = \frac{u_+^{(0)}}{\Delta u} = U^- - 1$ and drop the stars, then the nondimensional plain effective model of subsection II B takes the form

$$\partial_t u^+ = \nabla^2 u^+ - u^+ + U^+ + N^+, \quad y > q(x, t), \quad (12a)$$

$$\partial_t u^- =$$

$$D \nabla^2 u^- - K u^- + K U^- - N^-, \quad y < q(x, t), \quad (12b)$$

$$u^\pm = U^\pm + B^\pm H(x, t), \quad y = q(x, t), \quad (12c)$$

in addition to the nondimensional form of the front dynamics,

$$(u^- - u^+) \partial_t q = (-\partial_x q, 1) \cdot (\nabla u^+ - D \nabla u^-), \quad y = q(x, t). \quad (13)$$

III. LINEAR STABILITY ANALYSIS

A. Stationary state of the flat interface

Next, we investigate the stability of the flat interface $q(x, t) = \bar{q}$, without losing of generality, we may assume that $\bar{q} = 0$, also we assume that the concentration field is translational invariance along the x axis i.e., $u = \bar{u}(y)$. As a result, equations (12a-12c) take the form

$$\partial_y^2 \bar{u}^+ - \bar{u}^+ + U^+ + N^+ = 0, \quad y > 0, \quad (14a)$$

$$D \partial_y^2 \bar{u}^- - K \bar{u}^- + K U^- - N^- = 0, \quad y < 0, \quad (14b)$$

$$\bar{u}^\pm = U^\pm, \quad y = 0, \quad (14c)$$

recall that the local curvature vanishes in this case, $H = 0$. Equations (14a-14c) have the solutions,

$$\bar{u}^+ = U^+ + N^+ (1 - e^{-y}), \quad (15a)$$

$$\bar{u}^- = U^- - \frac{N^-}{K} \left(1 - e^{y \sqrt{K/D}}\right), \quad (15b)$$

notice that we apply the regularity condition $|u^\pm(\pm\infty)| < \infty$.

Considering the front dynamics in equations (10) and (13), we conclude that the flat front is stationary $v_n = 0$, and the influx is balanced by efflux across the flat interface $q = 0$,

$$\begin{aligned} \hat{\mathbf{n}} \cdot \mathbf{j}_- &= \hat{\mathbf{n}} \cdot \mathbf{j}_+ \Leftrightarrow \partial_y \bar{u}^+ = D \partial_y \bar{u}^- \Leftrightarrow \\ N^+ &= N^- \sqrt{\frac{D}{K}}. \end{aligned} \quad (16)$$

Equation (16) gives us the condition on the system parameters to achieve the stationary state and the coexistence of the two phases separated by the flat interface.

In view of equation (15a), we find that

$$N^+ = \bar{u}^+(y = \infty) - \bar{u}^+(y = 0), \quad (17)$$

therefore, N^+ resembles the excess concentration of the droplet material far from the droplet, as a result, we call N^+ the supersaturation parameter, which will play a central role in the next sections.

B. Dispersion relation

For investigating the stability of the flat front $q = 0$ and the stationary solutions (15a) and (15b), we introduce the disturbance,

$$u = \bar{u} + \hat{u}, \quad \bar{u} \gg \hat{u}, \quad (18a)$$

$$q = \bar{q} + \hat{q}, \quad \bar{q} \gg \hat{q}, \quad (18b)$$

then it holds that the curvature has the following expansion,

$$H(q) = \frac{\partial_x^2 q}{(1 + (\partial_x q)^2)^{3/2}} = \partial_x^2 \hat{q} + \dots$$

Substituting the perturbed solution (18a),(18b), in the system (12a)-(13), and neglecting nonlinear terms, we obtain the linearized problem of disturbances:

$$\partial_t \hat{u}^+ = \nabla^2 \hat{u}^+ - \hat{u}^+, \quad y > 0, \quad (19a)$$

$$\partial_t \hat{u}^- = D \nabla^2 \hat{u}^- - K \hat{u}^-, \quad y < 0, \quad (19b)$$

$$\hat{u}^\pm = B^\pm \partial_x^2 \hat{q} - \hat{q} \partial_y \bar{u}^\pm, \quad y = 0, \quad (19c)$$

$$\lim_{y \rightarrow \pm\infty} \hat{u}^\pm = 0, \quad (19d)$$

in addition to the flat interface disturbance equation,

$$\partial_t \hat{q} = \partial_y \hat{u}^+ - D \partial_y \hat{u}^- + (\partial_y^2 \bar{u}^+ - D \partial_y^2 \bar{u}^-) \hat{q}, \quad y = 0. \quad (20)$$

Here, we can introduce the normal modes,

$$\hat{u}^\pm(x, y, t) = A^\pm(y) e^{i\omega x + \sigma t}, \quad \hat{q}(x, t) = Q(\omega, \sigma) e^{i\omega x + \sigma t}, \quad (21)$$

where σ is the growth rate, and ω is the wave number of the disturbance. When substituting (21), in the linear system (19a)-(19d), one can find the solutions,

$$\hat{u}^+ = -Q(\omega^2 B^+ + N^+) \times \exp\left(-y\sqrt{\sigma + \omega^2 + 1} + i\omega x + \sigma t\right), \quad (22a)$$

$$\hat{u}^- = -Q\left(\omega^2 B^- + \frac{N^+}{D}\right) \times \exp\left(y\sqrt{\frac{\sigma}{D} + \omega^2 + \frac{K}{D}} + i\omega x + \sigma t\right). \quad (22b)$$

Putting these expressions (22a), (22b) in equation (20) yields the following dispersion relation,

$$\sigma = (\omega^2 B^+ + N^+) \sqrt{\sigma + \omega^2 + 1} + (\omega^2 D B^- + N^+) \sqrt{\frac{\sigma}{D} + \omega^2 + \frac{K}{D}} - N^+ \left(1 + \sqrt{\frac{K}{D}}\right), \quad (23)$$

notice that $\sigma = \omega = 0$ is a solution for (23) due to the flux balance (16). Now we will show that the dispersion equation (23) always has a unique positive solution for σ , as long as $\omega \neq 0$. For this purpose, we define the function

$$f(\sigma) = \sigma - (\omega^2 B^+ + N^+) \sqrt{\sigma + \omega^2 + 1} - (\omega^2 D B^- + N^+) \sqrt{\frac{\sigma}{D} + \omega^2 + \frac{K}{D}} + N^+ \left(1 + \sqrt{\frac{K}{D}}\right),$$

then it holds that,

$$(\omega^2 B^+ + N^+) \sqrt{\omega^2 + 1} + (\omega^2 D B^- + N^+) \sqrt{\omega^2 + \frac{K}{D}} > N^+ \left(1 + \sqrt{\frac{K}{D}}\right),$$

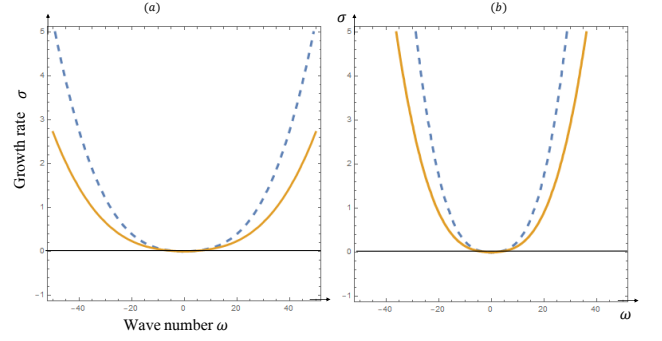


FIG. 4. (a) The dashed curve is the plot of the dispersion equation (23) of the two dimensional problem, while the solid curve is the plot of the dispersion equation (46) of the three dimensional problem. Both of them are for the parameter values of case I in Table (II), (b) the same but for the parameter values of case III.

that leads to $f(\sigma = 0) < 0$. On the other hand, we have $f(\sigma = +\infty) = +\infty$, therefore following the mean value theorem on the interval $0 < \sigma < \infty$, we conclude the existence of positive solution $\sigma > 0$ for equation (23), notice that this solution is unique in the limit $N^+ \ll 1$. As a result, the stationary flat interface solution is unstable as long as the system parameters obey the necessary condition (16). In comparison to the spherical droplet which can undergo three steady states as we mentioned in the introduction, the flat interface in our case can only undergo shape instability i.e., any small shape deformation will trigger elongation until interface division. This will be considered in depth in the next section.

Following (SI [1]) the authors provide examples of system parameter values of the effective model for which spherical droplets become unstable for five different cases. Here, we introduce cases I and III in Table I, which are based on measured values of liquid protein phases. One can check that these values indeed confirm the assumption (9). In addition, we add Table II for the corresponding nondimensional parameters (11). Although both cases do not satisfy the necessary condition (16), the plot of the dispersion equation (23) for these values exhibits unstable modes, see Fig (4).

IV. LONG WAVE NONLINEAR THEORY

In this section, we will develop our main finding, where we derive an amplitude like equation that governs the interface dynamics in the post linear (nonlinear) regime following Sivashinsky arguments [2]. This equation will be an asymptotic approximation in the limit of the small supersaturation number $N^+ \ll 1$.

First let us perform the shift transformations

$$u^+ \leftarrow u^+ + U^+ + N^+, \quad u^- \leftarrow u^- + U^- - N^-/K$$

	$D^- (\mu\text{m}^2/\text{s})$	$D^+ (\mu\text{m}^2/\text{s})$	$\gamma (\text{mN}/\text{m})$	$\beta^- = \beta^+ (\text{M} \cdot \text{m}^2/\text{N})$	$u_-^{(0)} (\text{mM})$	$u_+^{(0)} (\text{mM})$	$\nu^- (\text{mM}/\text{s})$	$\nu^+ (\text{nM}/\text{s})$	$k^- (1/\text{s})$	$k^+ (1/\text{s})$
Case I	10	10	10^{-3}	$2 \cdot 10^{-4}$	100	1	1	200	10^{-3}	10^{-3}
Case III	1	100	10^{-3}	$2 \cdot 10^{-4}$	100	1	10	$2 \cdot 10^5$	10^{-4}	1

TABLE I. For these parameters, the droplet interface becomes unstable. Both Cases are based on measured values of liquid protein phases, see (SI [1]) and reference therein.

	N^+	N^-	$B^- = B^+$	K	D	$(N^+)^{3/2}/B^+$
Case I	$2 \cdot 10^{-3}$	10.1	$2 \cdot 10^{-5}$	1	1	4.5
Case III	$2 \cdot 10^{-3}$	0.1	$2 \cdot 10^{-4}$	10^{-4}	10^{-2}	0.45

TABLE II. Values for some of the nondimensional parameters (11) that are related to Table I. The last column confirms the fact $(N^+)^{3/2}/B^+ = O(1)$.

on equations (12a)-(13) to obtain the system,

$$u_t^+ = u_{xx}^+ + u_{yy}^+ - u^+, \quad y > q(x, t), \quad (24a)$$

$$u^+ = -N^+ + B^+ H(x, t), \quad y = q(x, t), \quad (24b)$$

$$u_t^- = u_{xx}^- + u_{yy}^- - K u^-, \quad y < q(x, t), \quad (24c)$$

$$u^- = -\frac{N^-}{K} + B^- H(x, t), \quad y = q(x, t), \quad (24d)$$

$$\left(u^- - u^+ - \frac{N^-}{K} - N^+ + 1 \right) q_t = \quad (24e)$$

$$u_y^+ - D u_y^- - q_x (u_x^+ - D u_x^-), \quad y = q(x, t).$$

Then we introduce the curvilinear coordinates,

$$\tilde{y} = y - q(x, t), \quad \tilde{x} = x, \quad \tilde{t} = t,$$

and define,

$$q(x, t) = q(\tilde{x}, \tilde{t}) = \tilde{q}(\tilde{x}, \tilde{t}), \quad H(q) = \tilde{H}(\tilde{q})$$

$$u(x, y, t) = u(\tilde{x}, \tilde{y} + \tilde{q}(\tilde{x}, \tilde{t}), \tilde{t}) = \tilde{u}(\tilde{x}, \tilde{y}, \tilde{t}).$$

Applying the chain rule, and dropping the tildes, equations (24a)-(24e) are transformed into the form

$$u_t^+ - q_t u_y^+ = \quad (25a)$$

$$u_{yy}^+ + u_{xx}^+ + q_x^2 u_{yy}^+ - 2q_x u_{xy}^+ - q_{xx} u_y^+ - u^+, \quad y > 0,$$

$$u^+ = -N^+ + B^+ H(x, t), \quad y = 0, \quad (25b)$$

$$u_t^- - q_t u_y^- = \quad (25c)$$

$$D(u_{yy}^- + u_{xx}^- + q_x^2 u_{yy}^- - 2q_x u_{xy}^- - q_{xx} u_y^-) - K u^-, \quad y > 0,$$

$$u^- = \frac{N^-}{K} + B^- H(x, t), \quad y = 0, \quad (25d)$$

$$\left(u^- - u^+ - \frac{N^-}{K} - N^+ + 1 \right) q_t = \quad (25e)$$

$$(q_x^2 + 1) (u_y^+ - D u_y^-) - q_x (u_x^+ - D u_x^-), \quad y = 0.$$

Now we begin the scaling procedure of our fields, parameters, and variables. The last column of Table II confirms the scaling

$$B^\pm = O(N^{+3/2}).$$

For scaling the other parameters, we follow Sivashinsky scaling [2] to deduce the relations

$$\sigma = O(N^{+2}), \quad \text{and} \quad \omega = O(N^{+1/2}).$$

Therefore, let $0 < \varepsilon \ll 1$, then we define,

$$N^\pm = \varepsilon^2 \Lambda^\pm, \quad \sigma = \varepsilon^4 \Sigma, \quad \omega = \varepsilon \Omega, \quad B^\pm = \varepsilon^3 \Phi^\pm, \quad (26)$$

where all the Greek uppercase are $O(1)$. Substituting these scalings in the dispersion relation (23), we find that terms at order $O(\varepsilon^2)$ vanish due to the flux balance (16), while at the next order $O(\varepsilon^4)$, we obtain the scaled dispersion equation at the leading order,

$$\Sigma = \frac{\Lambda^+ \Omega^2}{2} \left(1 + \sqrt{\frac{D}{K}} \right), \quad (27)$$

which highlights the role of the nondimensional parameters (11).

Scaling (26) suggests the scaled variables

$$\tau = \varepsilon^4 t, \quad \xi = \varepsilon x, \quad \eta = y, \quad (28)$$

therefore the front dynamics are slow in time and wide in space. Motivated by the stationary solutions (15a)-(15b), we may assume the following asymptotic expansions of our fields,

$$u = \varepsilon^2 u_2(\xi, \eta, \tau) + \varepsilon^3 u_3 + \varepsilon^4 u_4 + \dots, \quad (29a)$$

$$q = q_0(\xi, \tau) + \varepsilon q_1 + \dots \quad (29b)$$

Next, we will substitute (29a) and (29b) in equations (25a)-(25e), and collect the terms of the same order.

At the leading order $O(\varepsilon^2)$, we obtain the system of equations which is equivalent to the base solutions that were considered in subsection III A,

$$u_{2\eta\eta}^+ - u_2^+ = 0, \quad \eta > 0,$$

$$u_2^+ = -\Lambda^+, \quad \eta = 0,$$

$$u_{2\eta\eta}^- - \frac{K}{D} u_2^- = 0, \quad \eta < 0,$$

$$u_2^- = \frac{\Lambda^-}{K}, \quad \eta = 0,$$

$$u_{2\eta}^+ - D u_{2\eta}^- = 0, \quad \eta = 0. \quad (30)$$

The solutions are,

$$u_2^+ = -\Lambda^+ e^{-\eta}, \quad u_2^- = \frac{\Lambda^-}{K} e^{\eta \sqrt{K/D}}, \quad (31)$$

then indeed, equation (30) is equivalent to the condition (16). At the next order $O(\varepsilon^3)$, the equations are homogenous therefore $u_3^\pm \equiv 0$.

At order $O(\varepsilon^4)$, we have the system,

$$\begin{aligned} u_{4\eta\eta}^+ - u_4^+ &= A_4^+ e^{-\eta}, \quad \eta > 0, \\ u_{4\eta\eta}^- - \frac{K}{D} u_4^- &= A_4^- e^{\eta\sqrt{K/D}}, \quad \eta < 0, \\ u_4^\pm &= 0, \quad \eta = 0, \\ q_{0\tau} &= u_{4\eta}^+ - D u_{4\eta}^-, \quad \eta = 0, \end{aligned} \quad (32)$$

where

$$\begin{aligned} A_4^+ &= \Lambda^+ (q_{0\xi}^2 + q_{0\xi\xi}) \\ A_4^- &= -\frac{\Lambda^-}{DK} \left(K q_{0\xi}^2 - \sqrt{DK} q_{0\xi\xi} \right), \end{aligned}$$

hence one can calculate the solutions,

$$u_4^+ = -\frac{A^+}{2} \eta e^{-\eta}, \quad u_4^- = \frac{A^-}{2} \sqrt{\frac{D}{K}} \eta e^{\eta\sqrt{K/D}}. \quad (33)$$

Substituting solutions (33) in equation (32) yields a closed form of the interface dynamics at the leading order,

$$\frac{\partial q_0}{\partial \tau} = -\lambda \frac{\partial^2 q_0}{\partial \xi^2}, \quad \lambda = \frac{1}{2} \left(\Lambda^+ + \frac{D}{K} \Lambda^- \right) > 0, \quad (34)$$

which is the desired asymptotic amplitude like equation that describes the evolution of the system in the post linear (nonlinear) regime. It is very remarkable that equation (34) is the known diffusion equation but with a negative coefficient which is not common in literature but exists in some physical systems.

If we go back to the original unscaled variable (x, t) , then equation (34) takes the form

$$\frac{\partial q_0}{\partial t} = -\lambda^* \frac{\partial^2 q_0}{\partial x^2}, \quad \lambda^* = \frac{N^+}{2} \left(1 + \sqrt{\frac{D}{K}} \right). \quad (35)$$

It is remarkable that most of the examples of the parameter values in (SI [1]) satisfy $K = D = 1$, in these cases equation (35) takes the following canonical form

$$\frac{\partial q_0}{\partial t} = -N^+ \frac{\partial^2 q_0}{\partial x^2}. \quad (36)$$

The solution of equation (34), with initial condition $q_0(\tau = 0) = A(\xi)$, is given via Fourier transform,

$$q_0(\xi, \tau) = \int_{-\infty}^{\infty} \frac{d\mu}{2\pi} \exp(i\mu\xi + \lambda\mu^2\tau) \int_{-\infty}^{\infty} dx e^{-ix\mu} A(x). \quad (37)$$

In this case, we cannot apply Fubini's theorem for switching the order of integration, since else we will obtain a divergent integral.

Similarly, one can calculate the next order $O(\varepsilon^5)$, and obtain the correction term of the front dynamics,

$$\frac{\partial q_1}{\partial \tau} = -\lambda \frac{\partial^2 q_1}{\partial \xi^2} - \varphi \frac{\partial^2 q_0}{\partial \xi^2}, \quad \varphi = \left(\Phi^+ + \sqrt{DK} \Phi^- \right), \quad (38)$$

notice that the curvature effect does not appear at the leading order, but it first appears here.

If we choose $\Lambda^+ = 1$ or $N^+ = \varepsilon^2$, then we may write equation (38) in the unscaled form,

$$\frac{\partial q_1}{\partial t} = -\lambda^* \frac{\partial^2 q_1}{\partial x^2} - \varphi^* \frac{\partial^2 q_0}{\partial x^2}, \quad \varphi^* = \frac{1}{\sqrt{N^+}} \left(B^+ + \sqrt{DK} B^- \right). \quad (39)$$

In the same manner, one can calculate the solution of equation (38) with the homogenous initial condition $q_1(\tau = 0) = 0$,

$$\begin{aligned} q_1(\xi, \tau) &= \\ \frac{\varphi\tau}{2\pi} \int_{-\infty}^{\infty} d\mu \mu^2 \exp(i\mu\xi + \lambda\mu^2\tau) \int_{-\infty}^{\infty} dx e^{-ix\mu} A(x). \end{aligned} \quad (40)$$

Next, we will find an exact solution for the interface equations (34) and (38) appended with special initial condition.

A. Special case of Gaussian initial condition

In order to model an almost flat initial interface for equation (34), as demonstrated in the schematic figure (Fig. 3), we may consider the following family of Gaussian initial conditions,

$$A(\xi) = -\sqrt{\alpha} e^{-\alpha\xi^2}, \quad \alpha > 0. \quad (41)$$

Since $1/\alpha^2$ resembles the width of the Gaussian Bell curve (41), we assume that $\alpha \ll 1$ to obtain an example of an almost flat interface.

Substituting the initial condition (41) in expression (37) yields an exact expression for the front in the leading order,

$$\begin{aligned} q_0(\xi, \tau) &= \frac{-1}{2\sqrt{\pi}} \int_{-\infty}^{\infty} d\mu \exp\left(i\mu\xi - \mu^2 \frac{1-4\alpha\lambda\tau}{4\alpha}\right) = \\ &= -\sqrt{\frac{\alpha}{1-4\alpha\lambda\tau}} \exp\left(-\frac{\alpha\xi^2}{1-4\alpha\lambda\tau}\right), \end{aligned} \quad (42)$$

notice that this solution is valid only for finite time regime, $0 \leq \tau < 1/(4\alpha\lambda)$. Consequently, we may consider $t_{dv} = 1/(4\alpha\lambda)$ as the time duration until droplet division. In dimensional formulation, it takes the form,

$$t_{dv} \sim \frac{\Delta u}{4\alpha [1 + (K/D)^{3/2}] \nu^+}, \quad (43)$$

notice that this law is *not universal*, rather, it depends on the initial interface $q(x, t = 0)$ or (41), due to its dependence on α .

In Fig. (5), we present the plots of the solution (42) for the parameters $\lambda = 1$ and $\alpha = 0.01$, hence $1/(4\alpha\lambda) = 25$, and for the time sequence $\tau = 0, 10, 22$. Indeed these solutions resemble the droplet division in the corresponding concentrated region as demonstrated in Fig. (3).

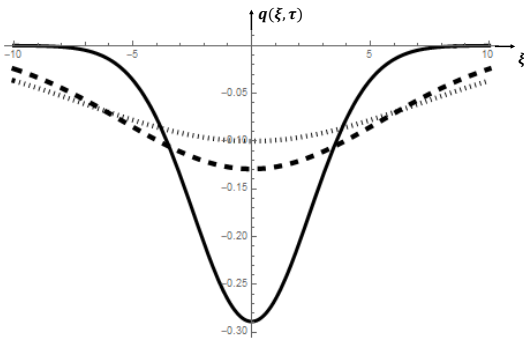


FIG. 5. Plots of the interface formula (42) with parameters $\lambda = 1$ and $\alpha = 0.01$. Dots for the initial condition $t = 0$, (41), dashes for $\tau = 10$, and solid for $\tau = 22$.

To find out the nature of the singular limit $\tau \rightarrow 1/(4\alpha\lambda)$, let us recall the following approximation in the distribution sense of the Dirac delta function

$$\delta_a(\xi) = \frac{e^{-(\xi/a)^2}}{\sqrt{\pi}|a|} \rightarrow \delta(\xi), \quad \text{as } a \rightarrow 0.$$

Consequently, if we define $a^2 = (1 - 4\alpha\lambda\tau)/\alpha$, then the solution (42) for the interface at the leading order manifests the following Dirac delta function singular limit,

$$q_0(\xi, \tau) = -\sqrt{\pi}\delta_a(\xi) \rightarrow -\sqrt{\pi}\delta(\xi). \quad \text{as } \tau \rightarrow 1/(4\alpha\lambda). \quad (44)$$

Similarly, the expression (40) for the correction term q_1 demonstrate the limit,

$$q_1(\xi, \tau) = -\frac{2\varphi\tau(a^2 - 2\xi^2)}{\lambda a^5} e^{-(\xi/a)^2} \sim \frac{2\varphi\tau\xi^2 e^{-(\xi/a)^2}}{\lambda a^5} \quad \text{as } \tau \rightarrow 1/(4\alpha\lambda), \quad (45)$$

which vanishes as $a \rightarrow 0$.

V. GENERALIZATION TO THE THREE DIMENSIONAL PROBLEM

The generalization of all the previous calculations to the three dimensional space is obviously straightforward due to consideration of symmetry and invariance. We replace the two dimensional spatial coordinate (x, y) with the three dimensional one (x_1, x_2, y) , hence we will have the spatial concentration field $u(x_1, x_2, y, t)$ and the interface surface $y = q(x_1, x_2, t)$. Recall that the local mean curvature of an explicit surface in the weak limit is given by

$$H(x_1, x_2, t) \sim \frac{1}{2}\nabla^2 q, \quad \nabla^2 = \partial_{x_1}^2 + \partial_{x_2}^2.$$

The dispersion relation (23) is replaced by,

$$\sigma = \left(\frac{\omega^2 B_+}{2} + N_+ \right) \sqrt{\sigma + \omega^2 + 1} + \left(\frac{\omega^2 D B_-}{2} + N_+ \right) \sqrt{\frac{\sigma}{D} + \omega^2 + \frac{K}{D}} - N_+ \left(1 + \sqrt{\frac{K}{D}} \right), \quad (46)$$

where the wave number $\omega^2 = \omega_1^2 + \omega_2^2$. Figure (4) provides plots for equation (46) with similar parameters values of Table (II).

For the nonlinear analysis, we obtain the following evolutionary equations of the leading and correction term for the two dimensional interface,

$$\partial_t q_0 = -\lambda^* \nabla^2 q_0, \quad (47a)$$

$$\partial_t q_1 = -\lambda^* \nabla^2 q_1 - \frac{1}{2} \varphi^* \nabla^2 q_0. \quad (47b)$$

Note that the initial condition (41) and the solution (42) of the one dimensional front may also be considered x_2 -translational invariance initial condition and solution for the two dimensional problem (47a).

VI. CONCLUSION

We investigate the interface of a chemical active droplet, close to the region where elongation begins until division, by formulating the effective model (12a)-(13) in the plain, and then stud in the linear and nonlinear regime. In the linear theory, we observe only one stationary state of the flat interface solution, this state is unstable of the kind shape instability, in comparison to the spherical droplet dynamics which may undergo three stationary states which we describe in the introduction. For the weak nonlinear theory, we develop an asymptotic equations slowly changing in time and wide in space, governing the evolution of the interface at the leading and correction order, where we consider the spatial and temporal scaling (28) of Sivashinsky that were discovered in the context of morphological instability of interface due to directional solidification of binary alloy [2]. In addition we employ the scaling $B^\pm = O(N^{+3/2})$ following Table (II) that is derived from the measured values in Table (I) which describes two real experimental setups considering liquid protein phases. Surprisingly, the evolution of the interface at the leading order (34), (35), (36) and (47a) is governed by the diffusion equation with a negative coefficient which is not common in literature but exists in some physical systems. Also we find that the curvature effect first appears in the interface correction terms (38), (39) and (47b). A typical example of Gaussian type initial condition (41), which is supposed to model an almost flat front, is appended to the interface equations (34) and (38), fortunately, an exact solution is obtained for the leading order (42) and the correction term (45). Indeed the plots of the leading order solution (42) resemble the evolution of the droplet division, Fig.

(5). This solution is valid only for a finite time regime, $0 \leq \tau < 1/(4\alpha\lambda)$, consequently, we obtain two main results, (i) an estimate for the time duration until droplet division $1/(4\alpha\lambda)$ or (43), which is *not universal* since it depends on the initial condition parameter α , (ii) the interface solution manifests Dirac delta function singularity (44) and (45) in the singular limit $\tau \rightarrow 1/(4\alpha\lambda)$. These results shed light on the nature of the division phenomena of the active droplet both in time and space. Due to considerations of symmetry and invariance, the generalization from the two dimensional to three dimensional problem is straightforward (Sec. V).

Future work will study the full effective model (8) with

bi-harmonic terms and compare it with the current study. This will be very reasonable since in both cases, we assume close proximity to the droplet interface.

ACKNOWLEDGEMENT

First, I thank God Almighty for His guidance.

I am indebted to Alexander A. Nepomnyashchy and Ehud Yariv for their support and patience. I thank Jörn Dunkel for introducing me to the inspiring work of the Max Planck Institute group [1], and I thank David Zwicker for helpful discussions.

-
- [1] D. Zwicker, R. Seyboldt, C. A. Weber, A. A. Hyman, and F. Jülicher, *Nature Physics* **13**, 408 (2017).
 [2] G. I. Sivashinsky, *Physica D* **8**, 243 (1983).
 [3] A. I. Oparin, *Origin of life* (Dover, 1952).
 [4] L. Giomi and A. DeSimone, *PRL* **112** (2014).
 [5] A. Z. Patashinski, R. Orlik, K. Paclawski, M. A. Ratner, and B. A. Grzybowski, *Soft Matter* **8**, 1601 (2012).
 [6] K. P. Browne, D. A. Walker, K. J. M. Bishop, and B. A. Grzybowski, *Angew. Chem. Int. Ed* **49**, 6756 (2010).
 [7] J. Macia and R. V. Sole, *Phil. Trans. R. Soc. B* **362**, 1821 (2007).
 [8] C. A. Weber, D. Zwicker, F. Jülicher, and C. F. Lee, arXiv **1806.09552v1** (2018).
 [9] W. J. Cahn and E. J. Hilliard, *J. Chem. Phys* **28**, 258 (1958).
 [10] D. Zwicker, *PhD Thesis: Physical Description of Centrosomes as Active Droplets* (Max Planck Institute for the Physics of Complex Systems, Dresden, 2013).